

Performance Analysis of Adaptive Physical Layer Network Coding for Wireless Two-way Relaying

Vijayaradharaj T. Muralidharan and B. Sundar Rajan

Dept. of ECE, IISc, Bangalore 560012, India, Email:{tmvijay, bsrajan}@ece.iisc.ernet.in

Abstract—The analysis of modulation schemes for the physical layer network-coded two way relaying scenario is presented which employs two phases: Multiple access (MA) phase and Broadcast (BC) phase. It was shown by Koike-Akino et. al. that adaptively changing the network coding map used at the relay according to the channel conditions greatly reduces the impact of multiple access interference which occurs at the relay during the MA phase. Depending on the signal set used at the end nodes, the minimum distance of the effective constellation at the relay becomes zero for a finite number of channel fade states referred as the singular fade states. The singular fade states fall into the following two classes: The ones which are caused due to channel outage and whose harmful effect cannot be mitigated by adaptive network coding are referred as the *non-removable singular fade states*. The ones which occur due to the choice of the signal set and whose harmful effects can be removed by a proper choice of the adaptive network coding map are referred as the *removable singular fade states*. In this paper, we derive an upper bound on the average end-to-end Symbol Error Rate (SER), with and without adaptive network coding at the relay, for a Rician fading scenario. It is shown that without adaptive network coding, at high Signal to Noise Ratio (SNR), the contribution to the end-to-end SER comes from the following error events which fall as SNR^{-1} : the error events associated with the removable singular fade states, the error events associated with the non-removable singular fade states and the error event during the BC phase. In contrast, for the adaptive network coding scheme, the error events associated with the removable singular fade states contributing to the average end-to-end SER fall as SNR^{-2} and as a result the adaptive network coding scheme provides a coding gain over the case when adaptive network coding is not used. It is shown that for a Rician fading channel, the error during the MA phase dominates over the error during the BC phase. Hence, adaptive network coding, which improves the performance during the MA phase provides more gain in a Rician fading scenario than in a Rayleigh fading scenario. Also, it is shown that for large Rician factors, among those removable singular fade states which have the same magnitude, those which have the least absolute value of the phase angle alone contribute dominantly to the end-to-end SER and it is sufficient to remove the effect of only such singular fade states.

I. BACKGROUND AND PRELIMINARIES

The wireless two-way relay channel (Fig. 1) in which bidirectional data transfer takes place between the nodes A and B with the help of the relay R is considered. All the three nodes are assumed to have half-duplex constraint, i.e., they cannot transmit and receive simultaneously in the same frequency band. The Denoise and Forward protocol, introduced in [1], is considered which consists of the following two phases: the *multiple access* (MA) phase, during which A and B simultaneously transmit to R and the *broadcast* (BC) phase during which R transmits to A and B. Network coding map,

also called the denoising map, is employed at R in such a way that A (B) can decode the message of B (A), given that A (B) knows its own message.

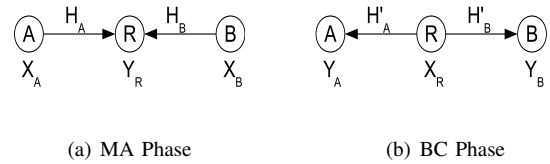


Fig. 1. The Two Way Relay Channel

A. Background

The concept of physical layer network coding has attracted a lot of attention in recent times. The idea of physical layer network coding for the two way relay channel was first introduced in [2], where the multiple access interference occurring at the relay was exploited so that the communication between the end nodes can be done using a two phase protocol. Information theoretic studies for the physical layer network coding scenario were reported in [3], [4]. A differential modulation scheme with analog network coding for bi-directional relaying was proposed in [5]. The design principles governing the choice of modulation schemes to be used at the nodes for uncoded transmission were studied in [6]. An extension for the case when the nodes use convolutional codes was done in [7]. A multi-level coding scheme for the two-way relaying scenario was proposed in [8]. Power allocation strategies and lattice based coding schemes for bi-directional relaying were proposed in [9].

Error analysis of the two-way AWGN relay channel with physical layer network coding based on the Detect and Forward (DF) protocol, in which the relay R transmits the estimate of the Exclusive OR (XOR) of A's and B's transmission bits, was done in [10]. Performance analysis for the two-way Rayleigh fading relay channel with physical layer network coding, based on the Amplify and Forward protocol was presented in [11]. For a two-way Rayleigh fading relay channel with BPSK modulation, upper and lower bounds on the Symbol Error Rate (SER) for the DF protocol were obtained in [12]. Exact BER analysis of the two-way Rayleigh fading relay channel with BPSK modulation for the DF protocol was done in [13].

While for BPSK modulation, the XOR network code offers the best performance, for other signal sets, changing the

network coding map adaptively according to channel conditions provides a significant performance improvement [6]. A computer search algorithm called the *Closest-Neighbour Clustering* (CNC) algorithm was proposed in [6] to obtain such adaptive network coding maps resulting in the best distance profile at R. An alternative procedure to obtain the adaptive network coding maps, based on the removal of deep channel fade conditions called singular fade states using Latin Squares was proposed in [14]. A quantization of the set of all possible channel realizations based on the network code used was obtained analytically in [15]. For the adaptive network coding schemes, performance improvement results due to a proper choice of adaptive network coding maps which effectively mitigate the effect of most of the singular fade states, referred as the removable singular fade states. In [14], a method to obtain adaptive network coding maps which remove the harmful effect of these removable singular fade states, using the completion of partially filled Latin Squares was proposed.

Unlike the DF protocol, in which XOR map is used irrespective of channel conditions, the average SER analysis of the adaptive network coding schemes proposed in [6], [14]-[15] should take into account the fact that the network coding maps used depend on the channel fade coefficients.

In this paper, we derive an upper bound on the end-to-end SER for the adaptive network coding schemes ([6], [14]-[15]) as well as for the case when adaptive network coding is not used, for a Rician fading scenario. With every singular fade state, we can associate an error event during the MA phase. It is shown that without adaptive network coding, at high Signal to Noise Ratio (SNR), the contribution to the end-to-end SER comes from the following error events which fall as SNR^{-1} : the error events associated with the removable singular fade states, the error events associated with the non-removable singular fade states and the error event during the BC phase. In contrast, for the adaptive network coding schemes proposed in [6] and [14]-[15], the error events associated with the removable singular fade states fall as SNR^{-2} and as a result the adaptive network coding schemes provide a coding gain over the case when adaptive network coding is not used. Also, it is shown that for sufficiently large Rician factors, only some of the removable singular fade states contribute dominantly to the end-to-end SER and it is sufficient to remove only such singular fade states.

B. Signal Model

Let \mathcal{S} denote the signal set of unit energy used at A and B, with $M = 2^\lambda$ points, λ being a positive integer. Assume that A (B) wants to transmit a λ -bit binary tuple to B (A). Let $\mu : \mathbb{F}_2^\lambda \rightarrow \mathcal{S}$ denote the mapping from bits to complex symbols used at A and B. Throughout the paper all the fading coefficients are assumed to be Rician distributed with a Rician factor K . A Rician distributed random variable X has a scattered component and a line of sight component, i.e., X can be written as $\frac{1}{\sqrt{K+1}}X_G + \sqrt{\frac{K}{K+1}}e^{j\theta}$, where X_G is a circularly symmetric complex Gaussian random variable with unit variance. Since θ is a constant, it can be cancelled out at

the transmitting nodes. Hence, without loss of generality, we assume $\theta = 0$.

Multiple Access (MA) phase: It is assumed that the CSI is not available at the transmitting nodes A and B during the MA phase. Also, a block fading scenario is assumed. Let $x_A = \mu(s_A)$, $x_B = \mu(s_B) \in \mathcal{S}$ denote the complex symbols transmitted by A and B respectively, where $s_A, s_B \in \mathbb{F}_2^\lambda$. The received signal at R is given by,

$$Y_R = H_A \sqrt{E_s} x_A + H_B \sqrt{E_s} x_B + Z_R,$$

where H_A and H_B are the fading coefficients associated with the A-R and B-R links respectively, which follow Rician distribution with a Rician factor K . Note that the Rician factor is the power ratio between the line of sight and scattered components. The additive noise Z_R is assumed to be $\mathcal{CN}(0, \sigma^2)$, where $\mathcal{CN}(0, \sigma^2)$ denotes the circularly symmetric complex Gaussian random variable with variance σ^2 . The average energy of A's and B's transmission is equal to E_s . Throughout, by SNR we mean the ratio $\frac{E_s}{\sigma^2}$. The ratio H_B/H_A denoted as $z = \gamma e^{j\theta}$, where $\gamma \in \mathbb{R}^+$ and $-\pi \leq \theta < \pi$, is referred as the *fade state* and for simplicity, also denoted by (γ, θ) .

Let $\mathcal{S}_R(H_A, H_B)$ denote the effective constellation seen at the relay during the MA phase, i.e.,

$$\mathcal{S}_R(H_A, H_B) = \{H_A x_A + H_B x_B | x_A, x_B \in \mathcal{S}\}.$$

Let $d_{\min}(H_A, H_B)$ denote the minimum distance between the points in the constellation $\mathcal{S}_R(H_A, H_B)$, i.e.,

$$d_{\min}(H_A, H_B) = \min_{\substack{(x_A, x_B), (x'_A, x'_B) \in \mathcal{S}^2 \\ (x_A, x_B) \neq (x'_A, x'_B)}} |H_A(x_A - x'_A) + H_B(x_B - x'_B)|. \quad (1)$$

Let $\Delta\mathcal{S}$ denote the difference constellation of the signal set \mathcal{S} , i.e., $\Delta\mathcal{S} = \{x - x' | x, x' \in \mathcal{S}\}$.

From (1), it is clear that there exists values of (H_A, H_B) for which $d_{\min}(H_A, H_B) = 0$. Whether for a given realization of (H_A, H_B) , $d_{\min}(H_A, H_B)$ is zero or not depends only on the fade state $\gamma e^{j\theta} = \frac{H_B}{H_A}$. The values of $\gamma e^{j\theta}$ for which $d_{\min}(H_A, H_B) = 0$ are of the form $-\frac{\Delta x_A}{\Delta x_B}$, where $\Delta x_A = x_A - x'_A$, $\Delta x_B = x_B - x'_B \in \Delta\mathcal{S}$ and are referred to as the singular fade states [14]. Note that 0 and ∞ are also singular fade states which occur when $H_B = 0$ or $H_A = 0$. Let \mathcal{H} denote the set of all singular fade states excluding 0 and ∞ .

Let $(\hat{x}_A^R, \hat{x}_B^R) \in \mathcal{S}^2$ denote the Maximum Likelihood (ML) estimate of (x_A, x_B) at R based on the received complex number Y_R , i.e.,

$$(\hat{x}_A^R, \hat{x}_B^R) = \arg \min_{(x'_A, x'_B) \in \mathcal{S}^2} |Y_R - H_A x'_A - H_B x'_B|. \quad (2)$$

Broadcast (BC) phase: Depending on the value of $\gamma e^{j\theta}$, R chooses a many-to-one map $\mathcal{M}^{\gamma, \theta} : \mathcal{S}^2 \rightarrow \mathcal{S}'$, where \mathcal{S}' is the signal set (of size between M and M^2) used by R during the BC phase. The elements in \mathcal{S}^2 which are mapped on to the same complex number in \mathcal{S}' by the map $\mathcal{M}^{\gamma, \theta}$ are said to

form a cluster. Let $\{\mathcal{L}_1, \mathcal{L}_2, \dots, \mathcal{L}_l\}$ denote the set of all such clusters. The formation of clusters for $\gamma^{j\theta}$ is called clustering, and is denoted by $\mathcal{C}^{\gamma,\theta}$. For examples of clusterings for 4-PSK and 8-PSK signal sets, see [14].

For a given realization of H_A and H_B , the choice of the network coding map depends only on the fade state $\gamma e^{j\theta} = \frac{H_B}{H_A}$, since all the distances between the points in the constellation $\mathcal{S}_R(H_A, H_B)$ can be normalized by H_A to make the set of all such distances a function of only $\gamma e^{j\theta}$.

The received signals at A and B during the BC phase are respectively given by,

$$Y_A = H'_A \sqrt{E_s} X_R + Z_A, \quad Y_B = \sqrt{E_s} H'_B X_R + Z_B, \quad (3)$$

where $X_R = \mathcal{M}^{\gamma,\theta}(\hat{x}_A, \hat{x}_B) \in \mathcal{S}'$ is the complex number transmitted by R. The fading coefficients corresponding to the R-A and R-B links, denoted by H'_A and H'_B respectively are Rician distributed with Rician factor K . The additive noises Z_A and Z_B are $\mathcal{CN}(0, \sigma^2)$. In order to ensure that A (B) is able to decode B's (A's) message, the clustering $\mathcal{C}^{\gamma,\theta}$ should satisfy the exclusive law [6], i.e.,

$$\left. \begin{aligned} \mathcal{M}^{\gamma,\theta}(x_A, x_B) &\neq \mathcal{M}^{\gamma,\theta}(x'_A, x_B), \text{ for } x_A \neq x'_A, \forall x_B \in \mathcal{S}, \\ \mathcal{M}^{\gamma,\theta}(x_A, x_B) &\neq \mathcal{M}^{\gamma,\theta}(x_A, x'_B), \text{ for } x_B \neq x'_B, \forall x_A \in \mathcal{S}. \end{aligned} \right\}$$

The node A (B) can decode the message of B (A) by observing Y_A (Y_B) through ML decoding, since A (B) knows x_A (x_B) and the map $\mathcal{M}^{\gamma,\theta}$ satisfies the exclusive law.

Definition 1: [14] The cluster distance between a pair of clusters \mathcal{L}_i and $\mathcal{L}_j, i \neq j$, is the minimum among all the distances calculated between the points $H_A x_A + H_B x_B$ and $H_A x'_A + H_B x'_B \in \mathcal{S}_R(H_A, H_B)$, where $(x_A, x_B) \in \mathcal{L}_i$ and $(x'_A, x'_B) \in \mathcal{L}_j$. The *minimum cluster distance* of the clustering $\mathcal{C}^{\gamma,\theta}$ is the minimum among all the cluster distances.

A clustering $\mathcal{C}^{\{h\}}$ is said to remove a singular fade state $h \in \mathcal{H}$, if the minimum cluster distance $d_{\min}(\mathcal{C}^{\{h\}})$ is greater than zero.

The CNC algorithm proposed in [6] obtains the map $\mathcal{M}^{\gamma,\theta}$ which results in the best distance profile during the MA phase at R, for a given $\gamma e^{j\theta}$. The CNC algorithm is run for all possible channel realizations and a partition of the set of all channel realizations is obtained depending on the chosen network coding map. For a given channel realization, the choice of the network coding map is indicated to A and B using overhead bits.

The CNC algorithm optimizes the entire distance profile instead of maximizing only the minimum distance. In some cases, this results in the use of signal sets with a larger cardinality during the BC phase and also results in an extremely large number of maps. For instance, for 16 QAM, the CNC algorithm results in more than 18,000 maps [6]. To solve this problem, an algorithm called the Nearest Neighbour Clustering (NNC) algorithm was proposed in [6] which maximizes the minimum distance alone, instead of optimizing the entire distance profile.

In [14], the equivalence between the network coding maps satisfying the exclusive law and the mathematical structure

called Latin Squares was shown. Network coding maps which remove all the singular fade states were obtained by the partial completion of Latin Squares.

Consider a singular fade state $h = -\frac{\Delta x_A}{\Delta x_B} \in \mathcal{H}$, where Δx_A and Δx_B are non-zero complex numbers which belong to $\Delta \mathcal{S}$. Let $\Delta x_A = x_A - x'_A$ and $\Delta x_B = x_B - x'_B$. Associated with the singular fade state h , we have the error event that the pair (x_A, x_B) is wrongly decoded as (x'_A, x'_B) . The CNC algorithm as well as the scheme proposed in [14] remove the singular fade state h by placing all such pairs (x_A, x_B) and (x'_B, x'_A) for which $\Delta x_A = x_A - x'_A$ and $\Delta x_B = x_B - x'_B$ in the same cluster.

The harmful effect of the singular fade states 0 and ∞ cannot be removed since the pairs (x_A, x_B) and (x_A, x'_B) (and also (x_A, x_B) and (x'_A, x_B)) result in these singular fade states and they cannot be placed in the same cluster without violating the exclusive law [6]. The singular fade states 0 and ∞ which occur due to channel outage, irrespective of the signal set used, are referred as the *non-removable singular fade states*. The rest of the singular fade states which depend on the signal set used are referred as the *removable singular fade states*. Henceforth, unless explicitly mentioned, by singular fade state, we refer to only the removable ones.

Throughout the paper, in a statement if it is mentioned simply as adaptive network coding, it refers to the scheme proposed in [6] as well as the one proposed in [14], i.e., the claim made in the statement holds for both the schemes.

In this paper, an upper bound on the average end-to-end SER is obtained for the two-way relaying scenario with and without adaptive network coding. From the obtained analysis, the reason why adaptive network coding provides performance improvement becomes very clear. Also, it is shown that not all the singular fade states contribute equally to the end-to-end error probability. Removing only those singular fade states which contribute dominantly to the end-to-end error probability reduces the system complexity at the relay as well as the number of overhead bits required for indicating the choice of the adaptive network coding map.

The contributions and organization of this paper are as follows:

- An upper bound on the average end-to-end SER for the wireless two-way relaying scenario with and without adaptive network coding is derived (Section II A and Section II B). It is shown that without adaptive network coding, at high SNR, the contribution to the average end-to-end SER comes from the following terms which decrease as SNR^{-1} : the error events associated with the removable and the non-removable singular fade states and the error event during the BC phase. In contrast, for the adaptive network coding schemes proposed in [6] and [14], the error events associated with the removable singular fade states fall as SNR^{-2} and as a result the adaptive network coding schemes provide a coding gain over the case when adaptive network coding is not used.
- It is shown that in a Rician fading scenario, the error during the MA phase dominates over the error during the

BC phase. Hence, the adaptive network coding schemes, which improve the performance during the MA phase, provides more gain in a Rician fading scenario than in a Rayleigh fading scenario (Section II).

- It is shown that in a Rician fading scenario, the removal of the singular fade state $s = 1$ assumes greatest significance. While in a Rayleigh fading scenario, all the singular fade states contribute dominantly to the overall average SER, it is shown that in a Rician fading scenario, for sufficiently large Rician factors, among those singular fade states which have the same magnitude, only those for which the absolute value of the phase angle is the least contribute dominantly to the end-to-end SER and it is sufficient to remove only such singular fade states (Section III).
- Simulation results which confirm the above mentioned facts are presented in Section IV.

Notations: $Q[\cdot]$ denotes the tail probability of the standard Normal distribution. $P_H\{E\}$ denotes the probability of the event E conditioning on the set of random variables H . $\mathbb{E}(X)$ denotes the expectation of X .

II. ERROR ANALYSIS OF THE WIRELESS TWO-WAY RELAYING SCENARIO

In the section, upper bounds on the end-to-end SER are obtained for the wireless two-way relaying scenario with and without adaptive network coding.

Let \hat{x}_B^A and \hat{x}_A^B denote the messages decoded by A and B respectively at the end of the BC phase. Let E_A and E_B respectively denote the error events $\hat{x}_B^A \neq x_B$ and $\hat{x}_A^B \neq x_A$. Let $H = (H_A, H_B, H'_A, H'_B)$ denote a particular realization of the channel fade coefficients. The end-to-end SER $P_H\{E_A \cup E_B\}$ given in (4), can be upper-bounded as in (5) (both shown at the top of the next page).

The first and second terms in (5), denoted as $P_H^{A,BC}$ and $P_H^{B,BC}$, are the probability of error events at node A and B respectively at the end of the BC phase, given that the relay decoded to the correct cluster during the MA phase. The third term in (5), denoted as P_H^{MA} , is the probability that the relay decodes to the wrong cluster during the MA Phase.

The choice of the signal set \mathcal{S}' used at R during BC phase depends on the number of clusters in the clustering $\mathcal{C}^{\gamma, \theta}$ [6], [14]. Let \mathcal{C}_{max} denote the clustering which has the maximum number of clusters over all possible $\gamma e^{j\theta}$ and let \mathcal{S}'_{max} denote the signal set associated with the clustering \mathcal{C}_{max} . Let $P^{A,BC} = \mathbb{E}(P_H^{A,BC})$ and $P^{B,BC} = \mathbb{E}(P_H^{B,BC})$. The upper-bound on the average error probability during the BC phase calculated for the case when R always uses the signal set \mathcal{S}'_{max} irrespective of $\gamma e^{j\theta}$ will serve as an upper-bound on $P^{A,BC}$ and $P^{B,BC}$ as well. Hence, we have,

$$P^{A,BC} = P^{B,BC} \leq e^{-K} \frac{1}{1 + \frac{\text{SNR } d_{min}^2(\mathcal{S}'_{max})}{4}},$$

where $d_{min}(\mathcal{S}'_{max})$ is the minimum distance of the signal set \mathcal{S}'_{max} .

The upper-bound on $P^{A,BC}$ and $P^{B,BC}$ given above is not tight. Since the performance advantage due to adaptive network coding is captured only by the term P_H^{MA} in (5), in the rest of the paper we do not focus on the probabilities $P^{A,BC}$ and $P^{B,BC}$.

The probability that the relay decodes to the wrong cluster during the MA Phase P_H^{MA} can be upper-bounded as,

$$P_H^{MA} \leq \sum_{(x'_A, x'_B): \mathcal{M}^{\gamma, \theta}(x'_A, x'_B) \neq \mathcal{M}^{\gamma, \theta}(x_A, x_B)} P_H\{(\hat{x}_A^R, \hat{x}_B^R) = (x'_A, x'_B)\}. \quad (6)$$

The probability $P_H\{(\hat{x}_A^R, \hat{x}_B^R) = (x'_A, x'_B)\}$ can be upper-bounded by the corresponding pair-wise error probability given by,

$$P_H^{MA}\{(x_A, x_B) \rightarrow (x'_A, x'_B)\} = Q \left[\frac{\sqrt{\text{SNR}} |H_A(x_A - x'_A) + H_B(x_B - x'_B)|}{\sqrt{2}} \right].$$

Hence, from (6), we get (7) (shown at the top of the next page), where $1_{\{c\}}$ is the indicator function which is one if the condition c is satisfied and is zero if it is not satisfied.

Averaging with respect to the fade coefficients in (7), we get (8) (shown at the top of the next page), where $\mathcal{R}\{(x_A, x_B), (x'_A, x'_B)\} \subseteq \mathbb{C}^2$ is the region

$$\{(H_A, H_B) : \mathcal{M}^{H_B/H_A}(x_A, x_B) \neq \mathcal{M}^{H_B/H_A}(x'_A, x'_B)\}.$$

Let $P^{MA}\{(x_A, x_B) \rightarrow (x'_A, x'_B)\}$ denote the term inside the summation in (8). In the following subsections upper bounds on $P^{MA}\{(x_A, x_B) \rightarrow (x'_A, x'_B)\}$ are obtained for the two-way relaying scenarios without and with adaptive network coding.

A. Two-way Relaying without Adaptive Network Coding

Consider the situation where R uses the same clustering \mathcal{C} which does not remove any of the singular fade states, for all values of $\gamma e^{j\theta}$. Since R uses the same clustering for all $\gamma e^{j\theta}$, the region $\mathcal{R}\{(x_A, x_B), (x'_A, x'_B)\}$ can be either null set or the entire \mathbb{C}^2 plane. If (x_A, x_B) and (x'_A, x'_B) are placed in the same cluster by the clustering \mathcal{C} , then the region is the null set and $P^{MA}\{(x_A, x_B) \rightarrow (x'_A, x'_B)\} = 0$. But since \mathcal{C} does not remove any of the singular fade states, for every singular fade state $-\frac{\Delta x_A}{\Delta x_B}, \Delta x_A, \Delta x_B \in \Delta \mathcal{S}$, there exists at least one pair of two-tuples $\{(x_A, x_B), (x'_A, x'_B)\}$ which satisfies $\Delta x_A = x_A - x'_A$ and $\Delta x_B = x_B - x'_B$ and for which (x_A, x_B) and (x'_A, x'_B) are not placed in the same cluster. For such pairs (x_A, x_B) and (x'_A, x'_B) , $\mathcal{R}\{(x_A, x_B), (x'_A, x'_B)\}$ is the entire \mathbb{C}^2 plane. For this case, the probability $P^{MA}\{(x_A, x_B) \rightarrow (x'_A, x'_B)\}$ defined in (6) is given in (9) (shown at the top of the next page). In (9), the suffix *FNC* indicates that fixed network coding is used at R, irrespective of the channel conditions. Also, in (9), $f(H_A)$ and $f(H_B)$ denote the probability density functions of the random variables H_A and H_B respectively. Substituting Rician probability density functions for $f(H_A)$

$$\begin{aligned}
P_H\{E_A \cup E_B\} &= P_H\{E_A \cup E_B | \mathcal{M}^{\gamma,\theta}(\hat{x}_A^R, \hat{x}_B^R) = \mathcal{M}^{\gamma,\theta}(x_A, x_B)\} P_H\{\mathcal{M}^{\gamma,\theta}(\hat{x}_A^R, \hat{x}_B^R) = \mathcal{M}^{\gamma,\theta}(x_A, x_B)\} \\
&\quad + P_H\{E_A \cup E_B | \mathcal{M}^{\gamma,\theta}(\hat{x}_A^R, \hat{x}_B^R) \neq \mathcal{M}^{\gamma,\theta}(x_A, x_B)\} P_H\{\mathcal{M}^{\gamma,\theta}(\hat{x}_A^R, \hat{x}_B^R) \neq \mathcal{M}^{\gamma,\theta}(x_A, x_B)\} \quad (4) \\
&\leq \underbrace{P_H\{E_A | \mathcal{M}^{\gamma,\theta}(\hat{x}_A^R, \hat{x}_B^R) = \mathcal{M}^{\gamma,\theta}(x_A, x_B)\}}_{P_H^{A,BC}} + \underbrace{P_H\{E_B | \mathcal{M}^{\gamma,\theta}(\hat{x}_A^R, \hat{x}_B^R) = \mathcal{M}^{\gamma,\theta}(x_A, x_B)\}}_{P_H^{B,BC}} + \underbrace{P_H\{\mathcal{M}^{\gamma,\theta}(\hat{x}_A^R, \hat{x}_B^R) \neq \mathcal{M}^{\gamma,\theta}(x_A, x_B)\}}_{P_H^{MA}}.
\end{aligned}$$

$$\begin{aligned}
P_H^{MA} &\leq \sum_{(x'_A, x'_B): \mathcal{M}^{\gamma,\theta}(x'_A, x'_B) \neq \mathcal{M}^{\gamma,\theta}(x_A, x_B)} Q \left[\frac{\sqrt{\text{SNR}} |H_A(x_A - x'_A) + H_B(x_B - x'_B)|}{\sqrt{2}} \right] \\
&= \sum_{(x'_A, x'_B): (x'_A, x'_B) \neq (x_A, x_B)} \left(\mathbf{1}_{\{\mathcal{M}^{\gamma,\theta}(x'_A, x'_B) \neq \mathcal{M}^{\gamma,\theta}(x_A, x_B)\}} Q \left[\frac{\sqrt{\text{SNR}} |H_A(x_A - x'_A) + H_B(x_B - x'_B)|}{\sqrt{2}} \right] \right), \quad (7)
\end{aligned}$$

$$P^{MA} \triangleq \mathbb{E}(P_H^{MA}) \leq \sum_{(x'_A, x'_B): (x'_A, x'_B) \neq (x_A, x_B)} \underbrace{\int \int_{\mathcal{R}\{(x_A, x_B), (x'_A, x'_B)\}} Q \left[\frac{\sqrt{\text{SNR}} |H_A(x_A - x'_A) + H_B(x_B - x'_B)|}{\sqrt{2}} \right] f(H_A) f(H_B) dH_A dH_B}_{P^{MA}\{(x_A, x_B) \rightarrow (x'_A, x'_B)\}}. \quad (8)$$

$$P_{FNC}^{MA}\{(x_A, x_B) \rightarrow (x'_A, x'_B)\} = \int \int_{\mathbb{C}^2} Q \left[\frac{\sqrt{\text{SNR}} |H_A(x_A - x'_A) + H_B(x_B - x'_B)|}{\sqrt{2}} \right] f(H_A) f(H_B) dH_A dH_B. \quad (9)$$

and $f(H_B)$, at high SNR, the integral given in (9) can be upper bounded as,

$$P_{FNC}^{MA}\{(x_A, x_B) \rightarrow (x'_A, x'_B)\} < \frac{e^{-K \left(\frac{|\Delta x_A + \Delta x_B|^2}{|\Delta x_A|^2 + |\Delta x_B|^2} \right)}}{\left(1 + \frac{\text{SNR}(|\Delta x_A|^2 + |\Delta x_B|^2)}{4} \right)}. \quad (10)$$

From (10), it can be seen that $P_{FNC}^{MA}\{(x_A, x_B) \rightarrow (x'_A, x'_B)\}$ decreases as SNR^{-1} at high SNR.

The probabilities $P^{A,BC}$ and $P^{B,BC}$ are proportional to e^{-K} at high SNR. If Δx_B belongs to $\Delta\mathcal{S}$, $-\Delta x_B$ also belongs to $\Delta\mathcal{S}$. For $\Delta x_A \neq 0$ and $\Delta x_B \neq 0$, one of the two $|\Delta x_A + \Delta x_B|^2$ and $|\Delta x_A - \Delta x_B|^2$, has to be less than $|\Delta x_A|^2 + |\Delta x_B|^2$. Hence, from (10), $P_{FNC}^{MA}\{(x_A, x_B) \rightarrow (x'_A, x'_B)\}$ is proportional to $e^{-\kappa K}$ where $\kappa < 1$, for some $x_A \neq x'_A$ and $x_B \neq x'_B$. When the Rician factor K increases, the contribution of the error during the BC phase to the overall average SER decreases and for large values of K , the contribution to the overall average SER comes totally from the error during the MA phase. The reason for this is that P_{BC}^A and P_{BC}^B (proportional to e^{-K}) decrease faster with K than those terms $P^{MA}\{(x_A, x_B) \rightarrow (x'_A, x'_B)\}$ which are proportional to $e^{-\kappa K}$ where $\kappa < 1$. For this reason, adaptive network coding, which improves the performance during the MA phase, provides more gain in Rician fading scenario than in a Rayleigh fading scenario, consistent with the simulation results in [6] and [15]. The exact reason why adaptive network coding improves the performance during the MA phase is described in the next subsection.

B. Two-way Relaying with Adaptive Network Coding

Consider the adaptive network coding schemes proposed in [6] and [14]. In both the schemes all the singular fade states are removed by a proper choice of the clustering.

Consider error events $(x_A, x_B) \rightarrow (x'_A, x'_B)$ at R for which $x_A = x'_A$ or $x_B = x'_B$. For such error events, the region $\mathcal{R}\{(x_A, x_B), (x'_A, x'_B)\}$ is the entire \mathbb{C}^2 since the pairs (x_A, x_B) and (x'_A, x_B) (and also the pairs (x_A, x_B) and (x_A, x'_B)) cannot be placed in the same cluster without violating the exclusive law. At high SNR, the probabilities $P^{MA}\{(x_A, x_B) \rightarrow (x_A, x'_B)\}$ and $P^{MA}\{(x_A, x_B) \rightarrow (x'_A, x_B)\}$ defined in (8) can be upper-bounded as,

$$P_{ANC}^{MA}\{(x_A, x_B) \rightarrow (x_A, x'_B)\} < \frac{e^{-K}}{1 + \frac{\text{SNR} |\Delta x_B|^2}{4}}, \quad (11)$$

$$P_{ANC}^{MA}\{(x_A, x_B) \rightarrow (x'_A, x_B)\} < \frac{e^{-K}}{1 + \frac{\text{SNR} |\Delta x_A|^2}{4}}. \quad (12)$$

The suffix *ANC* in the above two equations indicates that adaptive network coding is used at R.

Let $s = -\frac{\Delta x_A}{\Delta x_B}, \Delta x_A, \Delta x_B \neq 0 \in \Delta\mathcal{S}$ denote a singular fade state. For the adaptive network coding schemes proposed in [6] and [15], the complex fade state $(\gamma e^{j\theta})$ plane can be quantized into different regions depending on the clustering used at R. In the neighbourhood of every singular fade state, an associated region Γ_s exists in which a clustering which removes that singular fade state is used at R. For example, for the case when 4-PSK signal set is used at A and B, the quantization of the complex fade state plane is as shown in Fig. 2, along with the regions $R_1 - R_{12}$ associated with the 12 singular fade states [15]. The regions R_{13} and R_{14} in Fig. 2 are the clustering independent regions in which choice of the clustering does not matter and any clustering satisfying the exclusive law gives the same performance. For details, see [15].

Note 1: The quantization of the complex fade state plane is the same for 4-PSK signal set for the Nearest Neighbour

Clustering algorithm proposed in [14] and for the scheme proposed in [6], while it need not be the same for other signal sets. Nevertheless, for both the schemes, there exists a region in the neighbourhood of every singular fade state in which a clustering which removes that singular fade state will be used.

Let C_s denote the circle with the largest radius δ_s enclosed in the region Γ_s , with center at the singular fade state s . For example, for 4-PSK signal set, $s = 1 + j$ is a singular fade state and the circle C_{1+j} of radius δ_{1+j} enclosed in the region Γ_{1+j} (the region R_3) is as shown in Fig. 2.

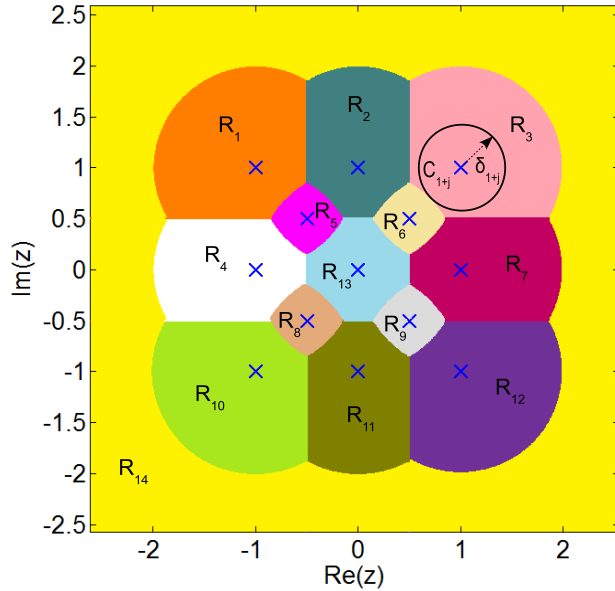


Fig. 2. The Diagram showing the fade state quantization for 4-PSK signal set

Let $\mathcal{E}(C_s)$ denote the region exterior to the circle C_s in the complex plane. If $\gamma e^{j\theta}$ lies inside the circle C_s , $\mathcal{M}^{\gamma,\theta}(x_A, x_B) = \mathcal{M}^{\gamma,\theta}(x'_A, x'_B)$. Hence, $\mathcal{R}\{(x_A, x_B), (x'_A, x'_B)\} \subset \{(H_A, H_B) : \frac{H_B}{H_A} \in \mathcal{E}(C_s)\} = \{(H_A, H_B) : |\frac{H_B}{H_A} + \frac{\Delta x_A}{\Delta x_B}| \geq \delta_s\}$. Hence, for the adaptive network coding schemes, the probability $P^{MA}\{(x_A, x_B) \rightarrow (x'_A, x'_B)\}$ defined in (8) can be upper-bounded as given in (13) (the suffix *ANC* in (13) indicates that adaptive network coding is used at R). Let $\Delta x_A = x_A - x'_A$ and $\Delta x_B = x_B - x'_B$. At high SNR, $P^{MA}_{ANC}\{(x_A, x_B) \rightarrow (x'_A, x'_B)\}$ can be upper-bounded as stated in the following theorem. Note that the bound is valid only at high SNR and is obtained by upper-bounding the term on the right hand side of (13).

Theorem 1: For $x_A \neq x'_A$ and $x_B \neq x'_B$, at high SNR $P^{MA}_{ANC}\{(x_A, x_B) \rightarrow (x'_A, x'_B)\}$ can be upper-bounded as given in (14) (shown at the top of the next page).

Proof: See Appendix. ■

From Theorem 1, it can be seen that for $x_A \neq x'_A$ and $x_B \neq x'_B$, at high SNR, $P^{MA}_{ANC}\{(x_A, x_B) \rightarrow (x'_A, x'_B)\}$ decreases as SNR^{-2} . But the overall diversity order of the end-to-end SER will be one, since $P^{MA}_{ANC}\{(x_A, x_B) \rightarrow (x_A, x'_B)\}$ and $P^{MA}_{ANC}\{(x_A, x_B) \rightarrow (x'_A, x'_B)\}$ given in (11) and (12) as well

as the probabilities $P^{A,BC}$ and $P^{B,BC}$ decrease as SNR^{-1} at high SNR.

Even though adaptive network coding does not provide any diversity advantage, it provides coding gain advantage over the case when adaptive network coding is not used. For the case when adaptive network coding is not used, from (10), it can be seen that $P^{MA}_{FNC}\{(x_A, x_B) \rightarrow (x'_A, x'_B)\}$ decreases as SNR^{-1} at high SNR, for all pairs (x_A, x_B) and (x'_A, x'_B) . In contrast for the adaptive network coding scheme, only those probabilities $P^{MA}_{ANC}\{(x_A, x_B) \rightarrow (x'_A, x'_B)\}$ for which $x_A = x'_A$ or $x_B = x'_B$ decrease as SNR^{-1} and the rest decrease as SNR^{-2} . In other words, for the adaptive network coding scheme, at high SNR, the pair-wise error events associated with the non-removable singular fade states 0 and ∞ decrease as SNR^{-1} and the pair-wise error events associated with the removable singular fade states decrease as SNR^{-2} . The adaptive network coding scheme provides coding gain advantage over the case when adaptive network coding is not used, by making the probability of the error events $(x_A, x_B) \rightarrow (x'_A, x'_B)$ for which $x_A \neq x'_A$ and $x_B \neq x'_B$ decrease as SNR^{-2} instead of SNR^{-1} .

From (10), for the case when adaptive network coding is not used, it follows that $P^{MA}_{FNC}\{(x_A, x_B) \rightarrow (x'_A, x'_B)\}$ is proportional to $e^{-K \frac{|1-s|^2}{1+|s|^2}}$. This suggests that removing certain singular fade states assumes more significance than removing the others and is discussed in the following section.

III. PARTIAL REMOVAL OF SINGULAR FADE STATES

In this section, it is shown that only some of the removable singular fade states contribute dominantly to the overall SER and only such singular fade states can be removed without a significant degradation in performance. Note that whether a singular fade state contributes significantly to the error probability depends on the Rician factor as well. For a Rayleigh fading scenario (Rician factor $K=0$), contributions of all the singular fade states to the overall SER are significant.

Since $P^{MA}_{FNC}\{(x_A, x_B) \rightarrow (x'_A, x'_B)\}$ is proportional to $e^{-K \frac{|1-s|^2}{1+|s|^2}}$, the factor $f(s) = \frac{|1-s|^2}{1+|s|^2}$, referred to as the *dominance factor* of the singular fade state s , determines whether the contribution from a singular fade state s is significant or not. The lesser the value of the dominance factor, the more the contribution of the singular fade state s to the SER. Since $f(s) = 0$ if and only if $s = 1$, *the removal of the singular fade state $s = 1$ assumes greatest significance*. Note that for the case when A and B use the same signal set, $s = 1$ will always be a singular fade state. Let $\angle s$ denote the phase angle of s . We have, $f(s) = 1 - \frac{2|s| \cos(\angle s)}{1+|s|^2}$.

Among those singular fade states which have the same absolute value $|s|$, those which have a lesser value of $|\angle s|$ ($|\angle s|$ ranges from 0 to π) have a lesser dominance factor and hence contribute more towards the overall SER. For sufficiently large Rician factors, among those singular fade states which lie on the same circle, R can choose to remove only those singular fade states which have the least absolute value of the phase angle.

$$P_{ANC}^{MA}\{(x_A, x_B) \rightarrow (x'_A, x'_B)\} \leq \int \int_{\{(H_A, H_B): \left| \frac{H_B + \frac{\Delta x_A}{\Delta x_B}}{H_A} \right| \geq \delta_s\}} Q \left[\frac{\sqrt{SNR} |H_A(x_A - x'_A) + H_B(x_B - x'_B)|}{\sqrt{2}} \right] f(H_A) f(H_B) dH_A dH_B. \quad (13)$$

$$P_{ANC}^{MA}\{(x_A, x_B) \rightarrow (x'_A, x'_B)\} \leq \frac{\exp \left\{ -2K + \frac{K(K+1) \left| 1 - \frac{\Delta x_A}{\Delta x_B} \right|^2}{\left[K+1 + SNR \frac{|\Delta x_B|^2}{4} \right] \delta_s^2 + (K+1) \left(1 + \frac{|\Delta x_A|^2}{|\Delta x_B|^2} \right)} \right\}}{\left(K+1 + SNR \frac{|\Delta x_B|^2}{4} \right) \left(\left[K+1 + SNR \frac{|\Delta x_B|^2}{4} \right] \delta_s^2 + (K+1) \left(1 + \frac{|\Delta x_A|^2}{|\Delta x_B|^2} \right) \right)} \quad (14)$$

Example 1: For the case when 4-PSK signal set is used at the nodes A and B, the twelve singular fade states are as shown in Fig. 3. For 4-PSK signal set, the dominance factor $f(s)$ for the 12 singular fade states are given by,

s	$f(s)$
1	0
$j, -1, -j$	1
$0.5 + 0.5j, 0.5 - 0.5j, 1 + j, 1 - j$	1/3
$-0.5 + 0.5j, -0.5 - 0.5j, -1 + j, -1 - j$	5/3

Among all the singular fade states, the singular fade state $s = 1$ is the most dominant one. Among those singular fade states which lie on the circle with radius $\frac{1}{\sqrt{2}}$, the singular fade states $0.5 + 0.5j$ and $0.5 - 0.5j$ are the dominant ones. Similarly, among those singular fade states which lie on the circle with radius $\sqrt{2}$, the singular fade states $1 + j$ and $1 - j$ are the dominant ones. The relay can choose to remove only the dominant singular fade states on each circle, which are the circled ones shown in Fig. 3.

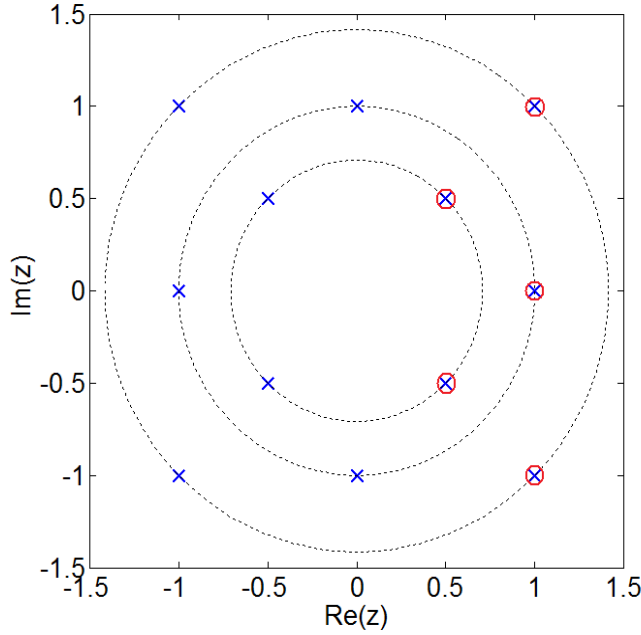


Fig. 3. The Diagram showing the dominant singular fade states for 4-PSK signal set

IV. SIMULATION RESULTS

The simulation results presented are for the case when the end nodes use 4-PSK signal set. The fading coefficient H_A, H_B, H'_A, H'_B are Rician distributed with a Rician factor $K = 4$ and unit variance. For comparison, we consider the case when R uses the Modulo-4 Latin Square shown in Fig. 5 irrespective of the channel condition (every entry of the Modulo-4 Latin Square is the modulo 4 addition of the row index and the column index). Note that the Modulo-4 Latin Square does not remove any of the 12 singular fade states. Fig. 4 shows the SNR vs BER plots for the different cases. From Fig. 4, it can be seen that the diversity order for all the cases considered is one. Also, it can be seen that at high SNR, the adaptive network coding scheme based on the removal of all the singular fade states using Latin Squares proposed in [14] provides nearly 8 dB gain over the case when Modulo-4 Latin Square is used irrespective of channel conditions. For details regarding the Latin Squares which remove the singular fade states, see [14].

Note 2: For 4-PSK signal set, the adaptive network coding scheme based on the removal of singular fade states proposed in [14] and the one based on the Nearest Neighbour Clustering algorithm proposed in [6] turn out to be the same.

Fig. 4 also shows the SNR vs BER plots for the case when only the singular fade state $s = 1$ is removed and for the case when all the singular fade states other than $s = 1$ are removed. Note that the bit-wise XOR network code removes the singular fade state $s = 1$ [14]. It can be seen that the SNR vs BER performance for both these cases are nearly the same. This means that the performance improvement provided by removing all the 11 singular fades states other than $s = 1$, is equal to the performance improvement provided by the removal of $s = 1$ alone. This confirms the assertion made earlier in Section III that the removal of the singular fade state $s = 1$ is of greatest significance. Fig. 4 shows the SNR vs BER plot for the case when only the five dominant singular fade states (the circled ones shown in Fig. 3) are removed. It can be seen from Fig. 4 that at high SNR, removing only the five dominant singular fade states results in nearly 7 dB performance improvement over the case when Modulo-4 Latin Square is used irrespective of channel conditions. In other words, at high SNR, the degradation in performance that results because of removing not all but only the dominant singular fade states is less than 1 dB.

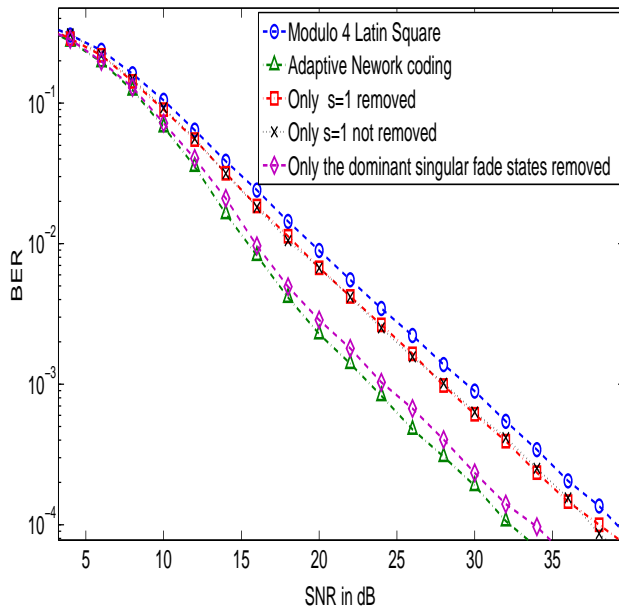


Fig. 4. SNR vs BER plots for the different schemes for Rician factor $K = 4$

	0	1	2	3
0	0	1	2	3
1	1	2	3	0
2	2	3	0	1
3	3	0	1	2

Fig. 5. The Modulo-4 Latin Square

V. DISCUSSION

An upper bound on the average end-to-end symbol error probability was obtained for the two-way relaying scenarios with and without adaptive network coding. From the analysis, the reason why adaptive network coding schemes provide performance improvement becomes clear. Also, it was shown that in a Rician fading scenario, some of the singular fade states contribute more to the average symbol error probability. Simulation results show that removing only such dominant singular fade states results in almost the same performance as that of the case when all the singular fade states were removed.

ACKNOWLEDGEMENT

This work was supported partly by the DRDO-IISc program on Advanced Research in Mathematical Engineering through a research grant as well as the INAE Chair Professorship grant to B. S. Rajan.

REFERENCES

- [1] P. Popovski and H. Yomo, "The AntiPackets Can Increase the Achievable Throughput of a Wireless MultiHop Network", IEEE ICC 2006, Istanbul, Turkey, June 2006.
- [2] S. Zhang, S. C. Liew and P. P. Lam, "Hot topic: Physical-layer Network Coding", ACM MobiCom '06, pp. 358–365, Sept. 2006.
- [3] S. J. Kim, P. Mitran and V. Tarokh, "Performance Bounds for Bidirectional Coded Cooperation Protocols", IEEE Trans. Inf. Theory, Vol. 54, pp. 5235–5241, Nov. 2008.

- [4] P. Popovski and H. Yomo, "Physical Network Coding in Two-Way Wireless Relay Channels", IEEE ICC, Glasgow, Scotland, June 2007.
- [5] L. Song, Y. Li, A. Huang, B. Jiao and A. V. Vasilakos, "Differential Modulation for Bidirectional Relaying With Analog Network Coding", IEEE Trans On Signal Processing, Vol. 58, No. 7, pp. 3933–3938, July 2010.
- [6] T. Koike-Akino, P. Popovski and V. Tarokh, "Optimized constellation for two-way wireless relaying with physical network coding", IEEE Journal on selected Areas in Comm., Vol. 27, pp. 773–787, June 2009.
- [7] T. Koike-Akino, P. Popovski and V. Tarokh, "Denosing strategy for convolutionally-coded bidirectional relaying", IEEE ICC 2009, Dresden, Germany, June 2009.
- [8] B. Hern and K. Narayanan, "Multilevel Coding Schemes for Compute-and-Forward", IEEE ISIT, St. Petersburg, Russia, July 2011.
- [9] M. P. Wilson and K. Narayanan, "Power Allocation Strategies and Lattice Based Coding schemes for Bi-directional relaying", IEEE ISIT, Seoul, Korea, July 2009.
- [10] K. Lu, S. Fu, Y. Qian and H.-H. Chen, "SER Performance Analysis for Physical Layer Network Coding over AWGN Channels, in Proc. of IEEE GLOBECOM 2009, Honolulu, HI, Nov. 2009.
- [11] R. H. Y. Louie, Y. Li, B. Vucetic, "Performance Analysis of Physical Layer Network Coding in Two-Way Relay Channels," in Proc. of IEEE GLOBECOM 2009, Honolulu, HI, Nov. 2009.
- [12] MinChul Ju and Il-Min Kim, "Error Performance Analysis of BPSK Modulation in Physical-Layer Network-Coded Bidirectional Relay Networks," IEEE Transactions On Comm., Vol. 58, No. 10, pp. 2770–2775, Oct. 2010.
- [13] M. Park, I. Choi and I. Lee, "Exact BER Analysis of Physical Layer Network Coding for Two-Way Relay Channels," IEEE Vehicular Technology Conference (VTC Spring) 2011, Yokohama, Japan, 15-18 May 2011.
- [14] Vishnu Nambodiri, Vijayaradharaj Muralidharan and B. Sundar Rajan, "Wireless Bidirectional Relaying and Latin Squares," Proceedings of IEEE Wireless Communications and Networking Conference (WCNC 2012), Paris, France, 1-4 April, 2012 (a detailed version of this paper is available in arXiv: 1110.0084v2 [cs.IT], 16 Nov. 2011).
- [15] Vijayaradharaj Muralidharan, Vishnu Nambodiri, and B. Sundar Rajan, "Channel Quantization for Physical Layer Network-Coded Two-Way Relaying," Proceedings of IEEE Wireless Communications and Networking Conference (WCNC 2012), Paris, France, 1-4 April, 2012 (a detailed version of this paper is available in arXiv: 1109.6101v2 [cs.IT], 16 Nov. 2011).
- [16] M. K. Simon and M.-S. Alouini, "Digital Communication over Fading Channels," 2nd edition, New York: Wiley, 2004.

APPENDIX

Before we prove Theorem 1, we prove the following lemma.

Lemma 1: For $c_0, r \in \mathbb{R}^+$ and $h_c \in \mathbb{C}$, the integral

$$I = \int_{\{h \in \mathbb{C}: |h| \geq c_0\}} e^{-r|h-h_c|^2} dh = \frac{1}{r} Q_1(\sqrt{2r}|h_c|, \sqrt{2r}c_0),$$

where Q_1 is the first order Marcum Q function. Also I can be upper bounded as,

$$I \leq \frac{1}{r} \frac{c_0}{c_0 - |h_c|} e^{-r(c_0 - |h_c|)^2}.$$

Proof: Let θ denote the phase angle of h and γ denote the absolute value of h .

Then the term inside the integral I can be written as,

$$e^{-r(\gamma^2 + |h_c|^2)} e^{2\gamma r |h_c| \cos(\theta - \phi)},$$

where $\phi = \tan^{-1}\left(\frac{\text{Im}(h_c)}{\text{Re}(h_c)}\right)$. Transforming h into polar coordinates (γ, θ) , the integral I can be written as,

$$I = \int_{\gamma=c_0}^{\infty} \gamma e^{-r(\gamma^2 + |h_c|^2)} \frac{1}{\pi} \int_{\theta=-\pi}^{\pi} e^{2\gamma r |h_c| \cos(\theta - \phi)} d\theta d\gamma. \quad (24)$$

$$I(H_A) = \int_{\left\{H_B: \left|H_B + \frac{H_A \Delta x_A}{\Delta x_B}\right| \geq |H_A| \delta_s\right\}} Q \left[\frac{\sqrt{\text{SNR}} |H_A(x_A - x'_A) + H_B(x_B - x'_B)|}{\sqrt{2}} \right] f(H_B) dH_B \quad (15)$$

$$\leq \frac{K+1}{\pi} \int_{\left\{H_B: \left|H_B + \frac{H_A \Delta x_A}{\Delta x_B}\right| \geq |H_A| \delta_s\right\}} \exp \left\{ -\frac{\text{SNR} |H_A \Delta x_A + H_B \Delta x_B|^2}{4} \right\} \exp \left\{ -(K+1) \left| H_B - \sqrt{\frac{K}{K+1}} \right|^2 \right\} dH_B \quad (16)$$

$$= \frac{K+1}{\pi} \int_{\left\{H'_B: |H'_B| \geq |H_A| \delta_s\right\}} \exp \left\{ -\left(K+1 + \frac{\text{SNR} |\Delta x_B|^2}{4} \right) \left| H'_B - \frac{(K+1)c}{\left[K+1 + \frac{\text{SNR} |\Delta x_B|^2}{4} \right]} \right|^2 \right\} \exp \left\{ -\frac{|c|^2 (K+1) \frac{\text{SNR} |\Delta x_B|^2}{4}}{K+1 + \frac{\text{SNR} |\Delta x_B|^2}{4}} \right\} dH'_B \quad (17)$$

$$\leq \frac{1}{\left[1 + K + \frac{\text{SNR} |\Delta x_B|^2}{4} \right]} \frac{\delta_s |H_A|}{\left[\delta_s |H_A| - \frac{(K+1)|c|}{K+1 + \frac{\text{SNR} |\Delta x_B|^2}{4}} \right]} \exp \left\{ -\left[1 + K + \frac{\text{SNR} |\Delta x_B|^2}{4} \right] \left(\delta_s |H_A| - \frac{(K+1)|c|}{K+1 + \frac{\text{SNR} |\Delta x_B|^2}{4}} \right)^2 \right\} \exp \left\{ -\frac{|c|^2 (K+1) \frac{\text{SNR} |\Delta x_B|^2}{4}}{K+1 + \frac{\text{SNR} |\Delta x_B|^2}{4}} \right\} \quad (18)$$

$$\approx \frac{1}{\left[1 + K + \frac{\text{SNR} |\Delta x_B|^2}{4} \right]} \exp \left\{ -\left[1 + K + \frac{\text{SNR} |\Delta x_B|^2}{4} \right] \delta_s^2 |H_A|^2 \right\} \exp \left\{ -|c|^2 (K+1) \right\} \quad (19)$$

$$P_{ANC}^{MA}(x_A, x_B) \rightarrow (x'_A, x'_B) \leq \frac{1}{K+1 + \frac{\text{SNR} |\Delta x_B|^2}{4}} \int_{H_A \in \mathbb{C}} \exp \left\{ -\left[K+1 + \frac{\text{SNR} |\Delta x_B|^2}{4} \right] \delta_s^2 |H_A|^2 \right\} \exp \left\{ -(K+1) \left| H_A \frac{\Delta x_A}{\Delta x_B} + \sqrt{\frac{K}{K+1}} \right|^2 \right\} \exp \left\{ -(K+1) \left| H_A - \sqrt{\frac{K}{K+1}} \right|^2 \right\} dH_A \quad (20)$$

$$= \frac{1}{K+1 + \frac{\text{SNR} |\Delta x_B|^2}{4}} \int_{H_A \in \mathbb{C}: |H_A| \geq 0} \exp \left\{ -2K + \frac{K(K+1)|1+s|^2}{\left[K+1 + \frac{\text{SNR} |\Delta x_B|^2}{4} \right] \delta_s^2 + (K+1)(1+|s|^2)} \right\} \exp \left\{ -\left(\frac{\left[K+1 + \frac{\text{SNR} |\Delta x_B|^2}{4} \right] \delta_s^2 + (K+1)(1+|s|^2)}{|1+s|^2} \right) \left| H_A(1+s) - \frac{\sqrt{K(K+1)}|1+s|^2}{\left[K+1 + \frac{\text{SNR} |\Delta x_B|^2}{4} \right] + (K+1)(1+|s|^2)} \right|^2 \right\} dH_A \quad (21)$$

$$= \frac{\exp \left\{ -2K + \frac{K(K+1)|1+s|^2}{\left[K+1 + \frac{\text{SNR} |\Delta x_B|^2}{4} \right] \delta_s^2 + (K+1)(1+|s|^2)} \right\}}{\left(K+1 + \frac{\text{SNR} |\Delta x_B|^2}{4} \right) \left(\left[K+1 + \frac{\text{SNR} |\Delta x_B|^2}{4} \right] \delta_s^2 + (K+1)(1+|s|^2) \right)} Q_1 \left[\sqrt{2 \left(\left[K+1 + \frac{\text{SNR} |\Delta x_B|^2}{4} \right] \delta_s^2 + (K+1)(1+|s|^2) \right)} \frac{\sqrt{K(K+1)}|1+s|}{\left[K+1 + \frac{\text{SNR} |\Delta x_B|^2}{4} \right] + (K+1)(1+|s|^2)}, 0 \right] \quad (22)$$

$$= \frac{\exp \left\{ -2K + \frac{K(K+1)|1+s|^2}{\left[K+1 + \frac{\text{SNR} |\Delta x_B|^2}{4} \right] \delta_s^2 + (K+1)(1+|s|^2)} \right\}}{\left(K+1 + \frac{\text{SNR} |\Delta x_B|^2}{4} \right) \left(\left[K+1 + \frac{\text{SNR} |\Delta x_B|^2}{4} \right] \delta_s^2 + (K+1)(1+|s|^2) \right)}. \quad (23)$$

Let I_0 denote the Bessel function of zeroth order of the first kind, i.e., (24) can be written as,

$$I = \frac{1}{r} \int_{\sqrt{2rc_0}}^{\infty} x e^{-\frac{1}{2}(x^2 + (\sqrt{2r}|h_c|)^2)} I_0[\sqrt{2r}|h_c|x] dx$$

$$= \frac{1}{r} Q_1(\sqrt{2r}|h_c|, \sqrt{2rc_0})$$

$$\leq \frac{1}{r} \frac{c_0}{c_0 - |h_c|} e^{-r(c_0 - |h_c|)^2}.$$

$$I_0(x) = \frac{1}{2\pi} \int_{-\pi}^{\pi} e^{-x \sin(\theta)} d\theta.$$

The above inequality follows from the fact that $Q_1(\alpha, \beta) \leq \frac{\beta}{\beta - \alpha} e^{-\frac{(\beta - \alpha)^2}{2}}$ [16]. ■

Using the transformation $x = \sqrt{2r}\gamma$, the integral I given in

PROOF OF THEOREM 1

Consider the integral $I(H_A)$ given in (15) (the equations (15)-(23) are shown at the top of the previous page). Substituting the Rician probability density function $f(H_B)$ in (15) and upper-bounding $Q(x)$ by $e^{-\frac{x^2}{2}}$, we get (16). Using the transformation $H'_B = H_B + H_A \frac{\Delta x_A}{\Delta x_B}$ in (16), we get (17), where $c = H_A \frac{\Delta x_A}{\Delta x_B} + \sqrt{\frac{K}{K+1}}$.

Using Lemma 1, the integral in (17) can be upper-bounded as given in (18). At high SNR, (18), can be approximated as in (19).

The upper bound on the probability $P_{ANC}^{MA}(x_A, x_B) \rightarrow (x'_A, x'_B)$ given in (13) can be written as,

$$P_{ANC}^{MA}(x_A, x_B) \rightarrow (x'_A, x'_B) = \int_{H_A \in \mathbb{C}} I(H_A) f(H_A) dH_A. \quad (25)$$

Substituting the Rician pdf $f(H_A)$, using (19), (25) can be upper bounded as given in (20). Rearranging the terms in (20) one gets (21), where $s = -\frac{\Delta x_A}{\Delta x_B}$. Using Lemma 1, the integral in (21) can be evaluated as given in (22). Since $Q_1(a, 0) = 1$ (22) can be simplified as in (23). This completes the proof.